

## MULTIPORT ANALYSIS BY PADÉ APPROXIMATION

G. Sener\*

Electronics and Communication Engineering Department, Cankaya University, 06810, Yenimahalle, Ankara, Turkey

**Abstract**—In this paper, a new method to analyze arbitrary shaped microstrip patch antennas is introduced. This method uses the multiport network model (MNM) together with a mathematical approximation called the “Padé approximation” such that the antenna input impedance obtained from the multiport analysis is approximated as a rational function of polynomials. Then, the roots of the denominator of this rational function are used to determine the antenna resonant characteristics. This new method is more time efficient than the standard multiport analysis because the evaluations are made at a single frequency. In the standard method, evaluations are made at multiple frequency values throughout the analysis. Results obtained by the new method are verified using the examples of rectangular and slot loaded compact microstrip patch antennas. Computational efforts for both procedures are presented.

### 1. INTRODUCTION

Analytical and numerical methods are used for the analysis of microstrip patch antennas. Some common analytical methods are the transmission line model [1–4], cavity model [5, 6], and multiport network model (MNM) [7, 8]. Numerical methods are the method of moments (MoM) [9–12], finite element method (FEM) [11, 12], and finite difference time domain method (FDTD) [13, 14]. The multiport network model can be considered an extension of the cavity model where the substrate is treated as a cavity surrounded by a perfect electric conductor (PEC) on the top and bottom planes, and a perfect magnetic conductor on side surfaces. Based on these assumptions, a

---

*Received 18 January 2012, Accepted 20 February 2012, Scheduled 28 February 2012*

\* Corresponding author: Goker Sener (sener@cankaya.edu.tr).

2D boundary value problem whose Green's function is expressed as a series expansion is defined. This analytical expression is a function of frequency and its terms are the modes of the resonator. In the multiport model, ports are placed around the patch periphery, and the Green's function is calculated at these multiports. During these calculations, the Green's function infinite series is truncated to the extent that the summation is sufficiently convergent to the true value. Once the Green's function is determined, the multiport impedance matrix can be obtained [15–17]. This impedance matrix defines the mutual and self-impedances among the ports and can be obtained analytically only for regularly-shaped patches such as rectangular, triangular and circular patches. For irregularly-shaped patches, such as those with slots, segmentation or de-segmentation methods are used [18–20]. In these methods, the overall patch geometry is divided into segments of regular shapes, and the composition or deduction of these regularly shaped patches is considered for segmentation or de-segmentation respectively.

Since the multiport network model is based on the solution of the Green's function with boundary assumptions, it offers accuracy and simplicity for the antenna analysis. However, it is not time efficient in wide band frequency simulations because the Green's function and the impedance matrix elements must be calculated at many frequency sweep values. In this paper, in order to speed up the multiport frequency analysis of microstrip patch antennas, the “Padé approximation” is used to approximate the antenna input impedance. The Padé approximation is a rational function of polynomials whose coefficients are obtained from the power series expansion of the approximated function [21]. To the author's knowledge, the application of Padé in microstrip structures is not new, and has been reported in F. Ling's paper [22] where the MoM solution of the microstrip structures is analyzed, and the frequency analysis over a broad band is expedited by the asymptotic waveform evaluation (AWE). In AWE, the power series coefficients (moments) are evaluated from a recursive relation, and then the Padé approximation is applied. The combination of AWE with MNM have been reported in several other papers as well. For example, the application of AWE to partitioned circuits is analyzed in [23]. The AWE technique is applied to interconnect structures characterized by sampled data in [24]. Nonlinear interconnect circuits are analyzed by the extension of the AWE technique in [25]. In this paper, the Padé approximation is used with the multiport network model specifically for the analysis of arbitrarily shaped microstrip patch antennas. In the multiport network model, the input impedance can be Padé approximated because the impedance expression is a

function of frequency and can be differentiated at a single expansion frequency. As a result, the frequency characteristics can be obtained by the roots of the denominator polynomial of the approximation which correspond to the antenna resonant frequencies (singularities of the input impedance). Part of this theory was presented earlier in a conference paper [26] where the impedance matrix elements were “vector Padé” approximated. In vector Padé approximation, the impedance matrix elements are approximated as rational functions with a common denominator. The poles of this approximation also yield antenna resonant frequencies, however the theory is applicable practically only for a few number of ports in the multiport model. Furthermore, the Padé approximation (scalar Padé) which is used in this paper is faster in the sense that it approximates the impedance port element only.

This paper presents the theory of multiport network model and segmentation in Sections 2 and 3, respectively. The theory of Padé approximation is presented in Section 4. The proposed method, Padé approximating the input impedance obtained from the multiport network model is described in Section 5. The validity and computational time advantage of the proposed method are presented in Section 6 through the examples of a rectangular and a slot loaded compact microstrip patch antenna.

## 2. THE MULTIPORT NETWORK MODEL

In the multiport network model for analyzing microstrip patch antennas, the patch is analyzed as a two-dimensional planar network. Multiple ports are located along the periphery. The length of each port should be small so that the field over this length is uniform. The number of ports depends on the field distribution along the edges. A greater number of ports should be chosen when there is a larger variation in the field distribution.

The impedance matrix corresponding to the ports is obtained by the Green’s function solution. The evaluation of the Green’s function is based on the cavity model where the region between the patch and the ground plane is treated as a cavity that is surrounded by magnetic walls around the periphery and by electric walls from the top and bottom sides. Since thin substrates are used, the field inside the cavity is treated as uniform along the thickness of the substrate. For a rectangular patch as in Fig. 1 with length  $L$  and width  $W$ , the Green’s function at an arbitrary point  $(x, y)$  for the rectangular patch with a  $z$ -directed electric current source at a point  $(x_0, y_0)$  is given

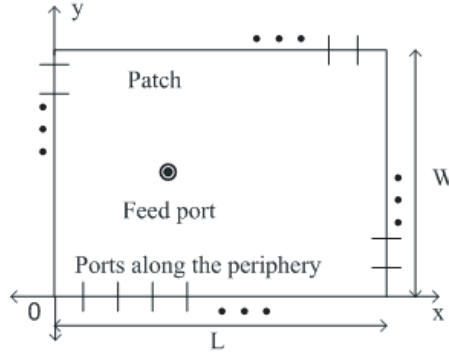


**Figure 1.** Multiport network model of a rectangular microstrip patch antenna.

by [7, 16, 17].

$$G(x, y/x_0, y_0) = \frac{j\omega\mu h}{LW} \sum_{m=0}^{\infty} \sum_{n=0}^{\infty} \frac{\sigma_m \sigma_n \cos(k_x x) \cos(k_y y) \cos(k_x x_0) \cos(k_y y_0)}{k_x^2 + k_y^2 - k^2} \quad (1)$$

where

$$\begin{aligned} k_x &= (m\pi)/L, & k_y &= (n\pi)/W \\ \sigma_m &= 1 \quad \text{if } m = 0, \quad \sigma_m = 2 \quad \text{otherwise} \\ k^2 &= \omega^2 \mu_0 \epsilon_0 \epsilon_r (1 - j\delta_e) \\ k_{mn}^2 &= k_x^2 + k_y^2 \end{aligned}$$

where  $h$  is the substrate thickness,  $\epsilon_r$  the effective dielectric constant, and  $\delta_e$  the loss tangent of the substrate.

Multiport impedance matrix elements  $Z_{ij}$  between the  $i$ th and the  $j$ th port of the patch are evaluated from the Green's function as

$$Z_{ij} = \frac{1}{W_i W_j} \int_{W_i} \int_{W_j} G(x_i, y_i/x_j, y_j) ds_i ds_j \quad (2)$$

where  $(x_i, y_i)$  and  $(x_j, y_j)$  denote the coordinates of the center point of the  $i$ th and  $j$ th ports of widths  $W_i$  and  $W_j$ , respectively.

The integral in (2) yields [7, 16, 17]

$$\begin{aligned} Z_{ij} &= \frac{j\omega\mu h}{LW} \sum_{m=0}^{\infty} \sum_{n=0}^{\infty} \frac{\sigma_m \sigma_n \cos(k_x x) \cos(k_y y) \cos(k_x x_0) \cos(k_y y_0)}{k_x^2 + k_y^2 - k^2} \\ &\quad \cdot \text{sinc}(k_x W_i/2) \text{sinc}(k_y W_j/2) \end{aligned} \quad (3)$$

It should be noted that the spectral wave numbers  $k_x$  and  $k_y$  that appear in the argument of cos and sinc functions refer to the

orientation of the ports. Therefore, (3) corresponds to a matrix entry where the  $i$ th port is along  $x$ -direction and the  $j$ th port is along the  $y$ -direction. Once the  $Z$ -matrix of the rectangular patch is obtained, the circuit configuration of any arbitrary shape patch can be analyzed by employing the segmentation method. In this method, the circuit pattern is obtained by combining the segments of regular shapes such as rectangles whose Green's function solutions are given in (1).

### 3. SEGMENTATION METHOD

For regularly shaped patches, rectangular, triangular or circular, the Green's function corresponding to the geometry under consideration is well known. In the analysis of irregular patches, whose Green's functions are not analytically available, the segmentation and/or desegmentation techniques are used in conjunction with the multiport analysis [18–20]. “Irregular shapes” refers to the microstrip antenna whose patch is cut in different shapes in order to fulfill a specific antenna property such as compactness, wideband characteristics and multiresonant operation.

Consider the patch structure shown in Fig. 2 where  $n$  segments are connected to create the overall patch geometry. In this network of  $n$ -segments,  $Z$ -matrices can be related to port voltages and currents by

$$\begin{bmatrix} \bar{V}_p \\ \bar{V}_c \end{bmatrix} = \begin{bmatrix} \tilde{Z}_{pp} & \tilde{Z}_{pc} \\ \tilde{Z}_{cp} & \tilde{Z}_{cc} \end{bmatrix} \begin{bmatrix} \bar{I}_p \\ \bar{I}_c \end{bmatrix} \tag{4}$$

where  $\bar{V}_p$ ,  $\bar{I}_p$  and  $\bar{V}_c$ ,  $\bar{I}_c$  are the voltages and currents at the  $p$  external and  $c$  internal ports. Furthermore, there are interconnection constraints on the  $c$  ports such that the voltages and currents are equal in magnitude, and the currents are in the opposite direction at the two

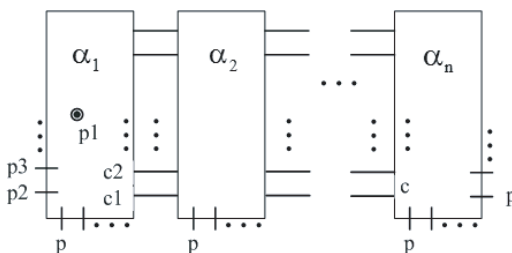


**Figure 2.** Segmentation of  $n$ -segments,  $\alpha_1, \alpha_n$ , to form the overall shaped patch segment.

connected ports. These constraints can be expressed as

$$\tilde{\Gamma}_1 \tilde{V}_c = \bar{0} \quad (5)$$

$$\tilde{\Gamma}_2 \tilde{I}_c = \bar{0} \quad (6)$$

where the  $\Gamma_1$  and  $\Gamma_2$  matrices describe these relations. In the  $\Gamma_1$  and  $\Gamma_2$  matrices, each row contains zeros that indicate a non-connection except the two columns that correspond to the two connected ports. Thus, the two nonzero entries in a row are 1 and  $-1$  for matrix  $\Gamma_1$  and both 1 for matrix  $\Gamma_2$ . Combining (4), (5), and (6), one can obtain the relation between  $I_p$  and  $I_c$  as

$$\begin{bmatrix} \tilde{\Gamma}_1 \tilde{Z}_{cc} \\ j\tilde{\Gamma}_2 \end{bmatrix} \tilde{I}_c = \begin{bmatrix} -\tilde{\Gamma}_1 \tilde{Z}_{cp} \\ \bar{0} \end{bmatrix} \tilde{I}_p \quad (7)$$

Substituting the value of  $\tilde{I}_c$ , obtained from (7) into (4), we get the overall network impedance matrix as

$$\tilde{Z}_p = \tilde{Z}_{pp} - \tilde{Z}_{pc} \begin{bmatrix} \tilde{\Gamma}_1 \tilde{Z}_{cc} \\ j\tilde{\Gamma}_2 \end{bmatrix}^{-1} \begin{bmatrix} \tilde{\Gamma}_1 \tilde{Z}_{cp} \\ \bar{0} \end{bmatrix}. \quad (8)$$

When the excitation port is defined as the first port of the matrix  $Z_p$ , then  $Z_{p11}$  is the input impedance of the antenna. Once the input impedance of the antenna is obtained, parameters such as the input reflection coefficient and the voltage standing wave ratio (VSWR) can be evaluated easily. The effect of fringe fields from the edges, surface waves and radiated waves are incorporated in the so called ‘‘edge admittance networks’’ containing equivalent impedances that are connected with the final antenna edge ports. Among the several formulations available in the literature to describe the edge admittances, a very common technique which is also used in this paper, is to increase the edge lengths by the ‘‘effective edge length’’ equivalent [17] to account for the stored energy in fringe fields.

In the following section, the Padé approximation is described for the purpose of approximating the elements of the impedance matrix in (8) as a rational function of polynomials.

#### 4. THE PADÉ APPROXIMATION

The Padé approximant of a function  $f(s)$  is the ratio of two polynomials with a numerator of degree  $p$  and a denominator of degree  $q$ , and denoted by the notation  $[p/q]$ . The approximation is obtained by equating the approximated function  $f(s)$  to its power series expansion up to a degree  $(p+q)$  [21], as shown in the following equation

$$f(s) \cong [p/q] = \frac{a_0 + a_1s + \dots + a_p s^p}{b_0 + b_1s + \dots + b_q s^q} = M_0 + M_1s + \dots + M_{p+q} s^{p+q} \quad (9)$$

where  $M'_n s$  are the  $n$ th moments of the series. By matching the two sides of (9), the coefficients in the numerator and denominator of the Padé approximation can be obtained from the following system of linear equations

$$\begin{bmatrix} M_p & M_{p-1} & \cdots & M_{p-q+1} \\ M_{p+1} & M_p & \cdots & M_{p-q+2} \\ \vdots & \vdots & \ddots & \vdots \\ M_{p+q-1} & M_{p+q} & \cdots & M_p \end{bmatrix} \begin{bmatrix} b_1 \\ b_2 \\ \vdots \\ b_q \end{bmatrix} = - \begin{bmatrix} M_{p+1} \\ M_{p+2} \\ \vdots \\ M_{p+q} \end{bmatrix} \quad (10)$$

and the numerator coefficients can be obtained from

$$a_r = \sum_{j=0}^r M_{r-j} b_j, \quad r = 0, 1, \dots, p. \quad (11)$$

If the power series is expanded at  $s_0$ , then the complex variable  $s$  in (9) has to be replaced by  $(s - s_0)$  and the moments in (10) and (11) have to be evaluated at  $s = s_0$ .

The Padé approximation in (9) can be applied to the impedance matrix entries of the multiport network model of a rectangular microstrip antenna given in (3) by replacing the  $j\omega$  term with the complex variable  $s$ . In the more general case of any arbitrary shaped microstrip patch antennas, including those with segmented structures, the procedure for obtaining the Padé approximation for the impedance elements is explained in the following section.

### 5. FORMULATION OF THE NEW PROCEDURE

Starting with the segmentation formulation for irregularly shaped microstrip patch antennas, the overall impedance matrix can be obtained from the sub-matrices of regular segments by

$$\tilde{Z}_p = \tilde{Z}_{pp} - \tilde{Z}_{pc} \begin{bmatrix} \tilde{\Gamma}_1 \tilde{Z}_{cc} \\ j\tilde{\Gamma}_2 \end{bmatrix}^{-1} \begin{bmatrix} \tilde{\Gamma}_1 \tilde{Z}_{cp} \\ \tilde{0} \end{bmatrix} \quad (12)$$

In order to Padé approximate the elements of the matrix  $Z_p$  in (12), its moments have to be known. Analytically, these moments can be obtained from the moments of the sub-matrices  $\tilde{Z}_{pp}$ ,  $\tilde{Z}_{pc}$ ,  $\tilde{Z}_{cc}$ ,  $\tilde{Z}_{dd}$ ,  $\tilde{Z}_{cp}$ . Since these sub-matrices belong to regularly shaped segments, their derivatives can be obtained through the Green's function analysis. Assuming all the impedance calculations and the moments are evaluated for the complex variable  $s = j\omega$ , then the  $n$ th derivative of the overall matrix can be written as

$$\frac{d^n}{ds^n}(\tilde{Z}_p) = (\tilde{Z}_{pp})^{(n)} - \left( \tilde{Z}_{pc} \begin{bmatrix} \tilde{\Gamma}_1 \tilde{Z}_{cc} \\ j\tilde{\Gamma}_2 \end{bmatrix}^{-1} \begin{bmatrix} \tilde{\Gamma}_1 \tilde{Z}_{cp} \\ \tilde{0} \end{bmatrix} \right)^{(n)} \quad (13)$$

where  $(n)$  stands for the  $n$ th partial derivative with respect to  $s$ . In (13), the  $n$ th derivative of the 2nd term on the right hand side can be written in the matrix form by the triple product rule as

$$\left( \tilde{Z}_{pc} \begin{bmatrix} \tilde{\Gamma}_1 \tilde{Z}_{cc} \\ j \tilde{\Gamma}_2 \end{bmatrix}^{-1} \begin{bmatrix} \tilde{\Gamma}_1 \tilde{Z}_{cp} \\ \tilde{0} \end{bmatrix} \right)^{(n)} = \sum_{k=0}^n \sum_{p=0}^k \binom{n}{k} \binom{k}{p} \tilde{Z}_{pc}^{(p)} \cdot \left( \begin{bmatrix} \tilde{\Gamma}_1 \tilde{Z}_{cc} \\ j \tilde{\Gamma}_2 \end{bmatrix}^{-1} \right)^{(k-p)} \left( \begin{bmatrix} \tilde{\Gamma}_1 \tilde{Z}_{cp} \\ \tilde{0} \end{bmatrix} \right)^{(n-k)} \quad (14)$$

where the terms  $\binom{n}{k}$  and  $\binom{k}{p}$  are the binomial coefficients. Furthermore, the derivative of the inverse matrix

$$\begin{bmatrix} \tilde{\Gamma}_1 \tilde{Z}_{cc} \\ j \tilde{\Gamma}_2 \end{bmatrix}^{-1} \quad (15)$$

can be evaluated by using the following matrix relation

$$\frac{d}{ds} (\tilde{Z}^{-1}) = -\tilde{Z}^{-1} \tilde{Z}^{(n)} \tilde{Z}^{-1} \quad (16)$$

When the derivatives are obtained analytically for the impedance matrix  $Z_p$ , the moments required for Padé approximation at the  $(i, j)$ th port can be evaluated from

$$M_{n(ij)} = \frac{Z_{p(ij)}^{(n)}(s) \Big|_{s=s_0}}{n!} \quad (17)$$

Once the elements of multiport impedance matrix  $Z_p$  are Padé approximated, the input impedance can be obtained from the corresponding feed port. By using the poles of the approximated input impedance expression, the antenna resonant characteristics can be determined.

The validity and time efficiency of the new method in comparison to the standard multiport analysis are experimented in the next section. First, a rectangular microstrip patch antenna with a single segment is analyzed. Second, a more complex slot loaded compact microstrip patch antenna with multiple segments is analyzed.

## 6. EXPERIMENTAL RESULTS

### 6.1. Example 1

Consider the rectangular patch configuration with its multiport model shown in Fig. 3. The patch dimensions are  $L = 8$  cm,  $W = 10$  cm, and

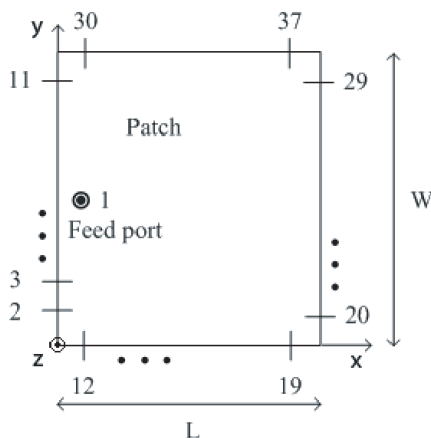


**Figure 3.** Multiport model of the rectangular patch antenna.

the substrate parameters are  $\epsilon_r = 4.3$ , thickness  $h = 0.159$  cm and loss tangent = 0.02. The feed port is located in the middle of the patch width and 0.1 cm away from the edge. The programming software Matlab is used for both the multiport analysis and the proposed method.

The simulation results are shown in Fig. 4 in the frequency interval 0.5–1.5 GHz. In Fig. 4(a), the  $x$  axis of the graph is the expansion frequency of the approximation, and the  $y$ -axis is the frequency obtained by the poles of the approximation of order [3/4]. The poles are evaluated and sorted by the algorithm called the “LAPACK — Linear Algebra Package” employed in Matlab. In this pole order, the last pole is observed to yield the best convergence. Hence, the 3rd and 4th pole frequencies are plotted, where it can be seen that the poles converge to required resonant frequencies in a band of the expansion frequency. Also, multiple poles converge to the same resonant frequency in the bandwidth of multiple pole convergence. In Fig. 4(b), the input reflection coefficient  $S_{11}$ (dB) obtained from the input impedance approximation is plotted against the frequency with three different expansion points. In Fig. 4(c), the new method and the standard multiport analysis results are compared.

In Fig. 5, the radiation pattern is shown at 0.88 GHz in the  $E$ -plane ( $\phi = 0^\circ$ ) and  $H$ -plane ( $\phi = 90^\circ$ ). The radiation is in the broadside direction, and HPBW in the  $E$  and  $H$  planes are  $170^\circ$  and  $85^\circ$  respectively. The co-polar components are  $E_\theta$  in the  $E$ -plane and  $E_\phi$  in the  $H$ -plane. The cross-polar components,  $E_\phi$  in the  $E$ -plane and  $E_\theta$  in the  $H$ -plane (not shown in the figure), are 34 dB and 40 dB

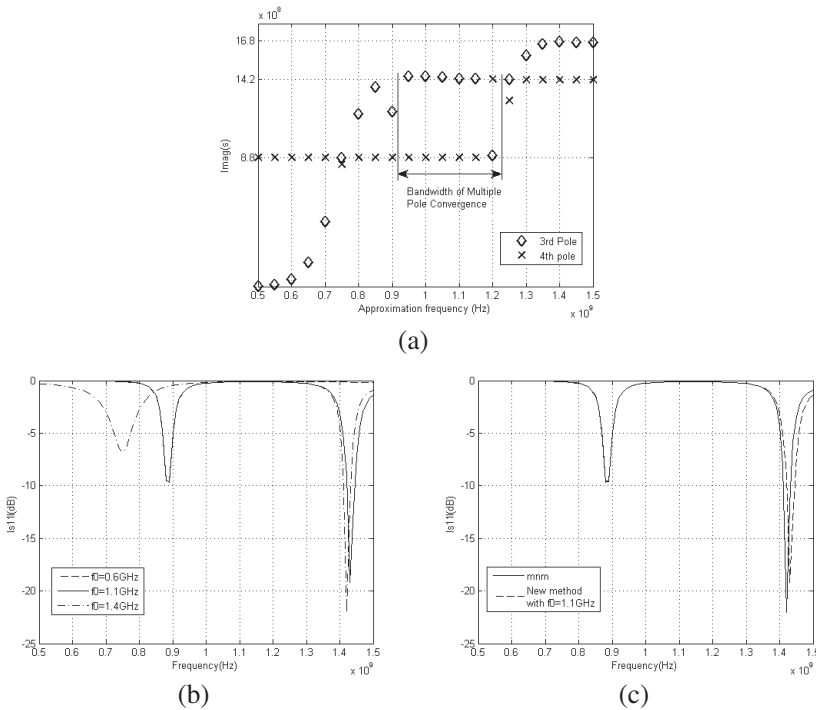


**Figure 4.** Rectangular microstrip patch antenna analysis. (a) Pole frequencies of the Padé approximated input impedance for order [3/4]. (b) Frequency analysis of the new method. (c) Comparison with mmm.

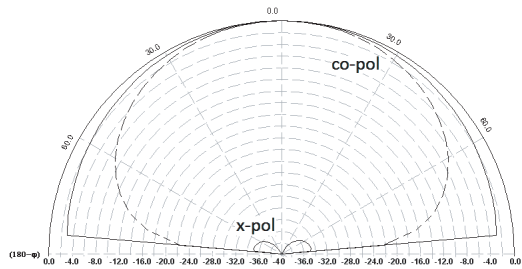


**Figure 5.** Normalized radiation pattern of the RMSA at 0.88 GHz; (—) *E*-plane co-polar and cross-polar and (---) *H*-plane co-polar.

less than the co-polar fields in the corresponding *E* and *H* planes.

Computational efforts in the frequency analysis of the rectangular patch antenna are presented in Table 1. The new method offers a

**Table 1.** Computational efforts in evaluating the frequency response of the rectangular patch antenna in the range 0.5–1.5 GHz for the standard MNM and the padé approximated MNM.

Number of Evaluations	Procedure of the Standard MNM (in seconds)	Procedure of the Approx. MNM (in seconds) for F[3/4]
100	0.11	-
1000	0.30	-
1	-	0.05

significant simulation time advantage over the conventional multiport analysis. The reason is that the Green's function and the impedance matrix elements are evaluated only once at the expansion frequency of the approximation. The weakness of the proposed method is that in order to converge to the desired resonant characteristics, the expansion frequency must be chosen close to the actual resonant frequency of the antenna. Therefore, a prior expectation of the frequency characteristics is required before the analysis. To compensate this weakness and enable wider frequency response, higher order approximations can be used. As can be seen from Fig. 4(a), high order approximations provide more poles to contribute to the convergence, and the convergence bandwidth increases. However, in such a case, the computation time required to evaluate moments also increases. If we call the degree of the numerator and denominator of the approximation  $p$  and  $q$  respectively,  $p+q$  evaluation of the moments is necessary to find the approximation. Therefore, if the time required for  $p+q$  evaluations exceeds the computation time for the standard analysis, the time advantage of the proposed method disappears. In view of all these considerations, to obtain a precise formulation for the simulation time is difficult. Nevertheless, the approximation order [3/4] yields approximately a 20% multiple band of convergence and the frequency simulations show good agreement with the standard method.

In the next example, a slotted compact patch antenna is used. Because of the slot on the patch, this antenna is considered to be irregularly shaped where the analytic solution of the Green's function is not available. Therefore, the multiport model of the patch contains segmented structures.

## 6.2. Example 2

A slot loaded compact microstrip patch antenna can be obtained from a rectangular microstrip antenna by cutting a slot from one of its non radiating edges. The purpose of this antenna is to obtain lower resonant frequencies at small dimensions. The resonant frequency is decreased because the surface currents travel longer distances due to the slot. Since the Green's function solution is not readily available, the segmentation method can be used by utilizing three rectangular segments. The multiport model of the patch is shown in Fig. 6 with dimensions  $L = 6$  cm,  $W = 4$  cm,  $W_s = 2$  cm,  $L_s = 2$  cm,  $x = 0.25$  cm and the substrate parameters  $\epsilon_r = 2.33$ ,  $h = 0.159$  cm and loss tangent = 0.002. This is the same antenna simulation used by Kumar and Ray in [17], where the resonant frequency as that of the rectangular patch without the slot is 1.60 GHz and, when the slot is introduced, the resonant frequency is decreased to 1.14 GHz.

The simulation results are shown in Fig. 7. In parts (a) and (b), the pole frequencies at order  $[3/4]$  are plotted with respect to the expansion frequencies in the frequency range 1–1.25 GHz and 0.8–3 GHz respectively. The resonant frequencies are indicated by dot-lines at 1.14, 2.35 and 2.70 GHz. In part (c), the frequency analysis results show that the new method is accurate provided that the expansion frequency is within the bandwidth of convergence. In Fig. 8, the radiation pattern is shown. The cross-polar electric field components are increased due to the slot, yet they remain 16 dB and 28 dB less than the corresponding co-polar fields in the  $E$  and  $H$  planes. The radiation is broadside, and the HPBW in the  $E$  and  $H$  planes are  $96^\circ$  and  $90^\circ$  respectively.

Time efforts are shown in Table 2. Where the advantage of the proposed method is more significant than the one in the previous

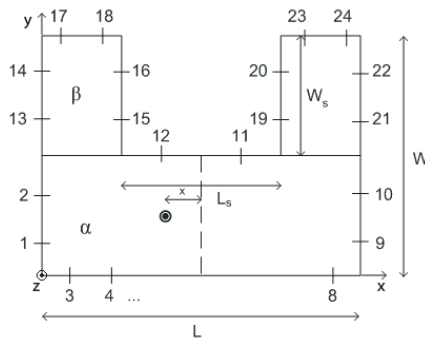


**Figure 6.** Multiport model of the slot loaded compact microstrip patch antenna.

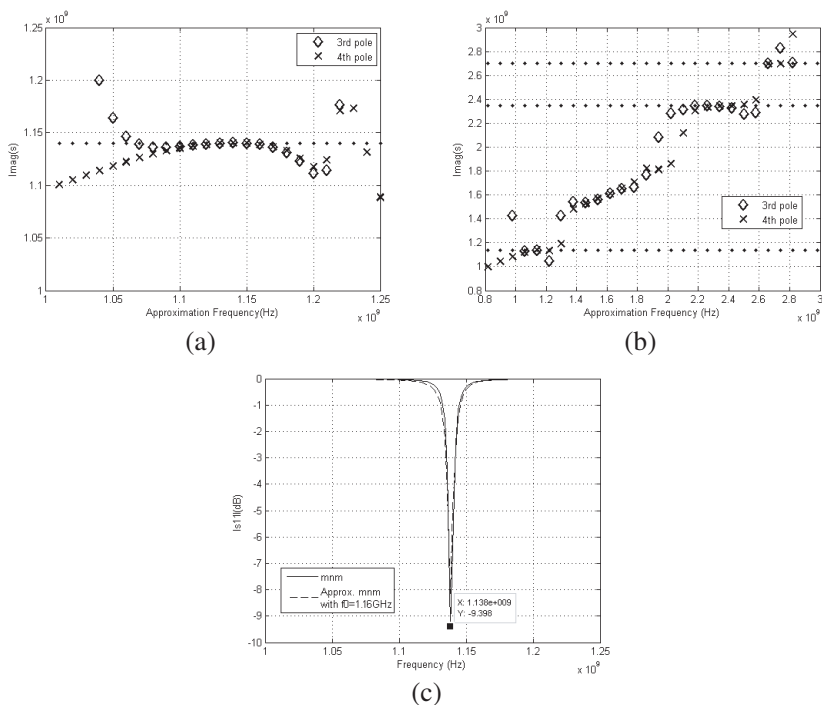


**Figure 7.** Slot loaded compact microstrip patch antenna analysis. (a) Pole frequencies of the Padé approximated input impedance for order [3/4]. (b) Pole frequencies in the range 0.8–3 GHz. (c) Frequency analysis of the new method in comparison with mmm.

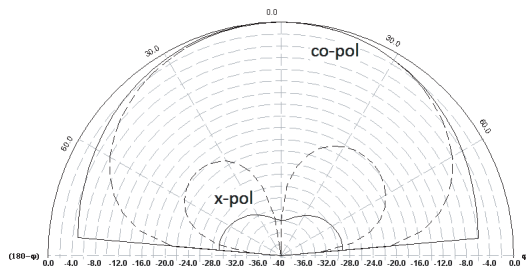


**Figure 8.** Normalized radiation pattern of the slot loaded compact microstrip patch antenna at 1.14 GHz; (—)  $E$ -plane co-polar and cross-polar and (---)  $H$ -plane co-polar and cross-polar.

example. The reason is that in multiport analysis there are extra evaluations of the Green’s function and the impedance matrices for the segmented structures at each frequency step.

**Table 2.** Computational efforts in evaluating the frequency response of the slot loaded compact MS antenna in the range 1–1.25 GHz for the standard MNM and the padé approximated MNM.

Number of Evaluations	Procedure of the Standard MNM (in seconds)	Procedure of the Approx. MNM (in seconds) for F[3/4]
100	9.32	-
1	-	0.39

## 7. CONCLUSION

A new method for the analysis of arbitrary shaped microstrip patch antennas has been proposed. Through the examples of rectangular and slot loaded compact microstrip patch antennas, the new method is observed to be more time efficient than the standard multiport analysis, because it uses a single rational function in order to obtain the antenna frequency characteristics. The major limitation of the method is the restricted convergence band for determining the expansion frequency. Although higher order approximations can be used to enlarge this bandwidth, the simulation time advantage starts to diminish as more calculations of derivatives are involved. Alternatively, multiple expansion points can be used to enlarge the convergence band in the analysis [22]. The efficiency regarding the two methods depends on the frequency band of the analysis. As the frequency band increases, the multiple expansion point approach may be preferred because the evaluation of higher order derivatives causes numerical instability problems besides the decrease in time efficiency.

## REFERENCES

1. Carver, K. R. and J. W. Mink, "Microstrip antenna technology," *IEEE Transactions on Antennas and Propagation*, Vol. 29, No. 1, 2–24, January 1981.
2. Kasabegouadar, V. G., "Low profile suspended microstrip antennas," *Journal of Electromagnetic Waves and Applications*, Vol. 25, No. 13, 1795–1806, 2011.
3. Fallahzadeh, S. and M. Tayarani, "A new microstrip UWB bandpass filter using defected microstrip structures," *Journal of Electromagnetic Waves and Applications*, Vol. 24, No. 7, 893–902, 2010.

4. Kashwan, K. R., V. Rajeshkumar, T. Gunasekaran, and K. R. Kumar, "Design and characterization of pin fed microstrip patch antennae," *2011 Eighth International Conference on Fuzzy Systems and Knowledge Discovery (FSKD)*, Vol. 4, 2258–2262, 2011.
5. Lo, Y. T., D. Solomon, and W. F. Richards, "Theory and experiment on microstrip antennas," *IEEE Transactions on Antennas and Propagation*, Vol. 27, No. 2, 137–145, 1979.
6. Akdagli, A. and A. Toktas, "A novel expression in calculating resonant frequency of H-shaped compact microstrip antennas obtained by using artificial bee colony algorithm," *Journal of Electromagnetic Waves and Applications*, Vol. 24, No. 14–15, 2049–2061, 2010.
7. Okoshi, T. and T. Miyoshi, "The planar circuit — An approach to microwave integrated circuitry," *IEEE Transactions on Microwave Theory Tech.*, Vol. 20, 245–252. April 1972.
8. Palanisamy, V. and R. Garg, "Analysis of arbitrarily shaped microstrip patch antennas using segmentation technique and cavity model," *IEEE Transactions on Antennas and Propagation*, Vol. 34. No. 10, October 1986.
9. Pergol, M. and W. Zieniutycz, "Rectangular microstrip resonator illuminated by normal-incident plane wave," *Progress In Electromagnetics Research*, Vol. 120, 83–97, 2011.
10. Ling, J., S. Gong, S. Qin, W. Wang, and Y. Zhang, "Wide-band analysis of on-platform antenna using MoM-PO combined with Maehly approximation," *Journal of Electromagnetic Waves and Applications*, Vol. 24, No. 4, 475–484, 2010.
11. Chen, Y., S. Yang, S. He, and Z.-P. Nie, "Fast analysis of microstrip antennas over a frequency band using an accurate MoM matrix interpolation technique," *Progress In Electromagnetics Research*, Vol. 109, 301–324, 2010.
12. Chen, Y., S. Yang, S. He, and Z. Nie, "Efficient analysis of wireless communication antennas using an accurate [Z] matrix interpolation technique," *International Journal of RF and Microwave Computer-Aided Engineering*, Vol. 20, No. 4, 382–390, 2010.
13. Yang, S., Y. Chen, and Z.-P. Nie, "Simulation of time modulated linear antenna arrays using the FDTD method," *Progress In Electromagnetics Research*, Vol. 98, 175–190, 2009.
14. Luo, Z., X. Chen, and K. Huang, "A novel electrically-small microstrip genetic antenna," *Journal of Electromagnetic Waves and Applications*, Vol. 24, No. 4, 513–520, 2010.

15. Okoshi, T., *Planar Circuits for Microwave and Lightwaves*, Springer-Verlag, New York, 1985.
16. James, J. R. and P. S. Hall, *Handbook of Microstrip Antennas*, 455–522, Artech House, 2003.
17. Kumar, G. and K. P. Ray, *Broadband Microstrip Antennas*, 383–401, Artech House, 2003.
18. Chadha, R. and K. C. Gupta, “Segmentation method using impedances matrices for analysis of planar microwave circuits,” *IEEE Transactions on Microwave Theory and Techniques*, Vol. 29, No. 1, January 1981.
19. Gupta, K. C. and P. C. Sharma, “Segmentation and desegmentation techniques for analysis of microstrip antennas,” *IEEE Antennas and Propagation Society International Symposium*, Vol. 19, 1981.
20. Sharma, P. C. and K. C. Gupta, “Desegmentation method for analysis of two dimensional microwave circuits,” *IEEE Transactions on Microwave Theory and Techniques*, Vol. 29, No. 10, October 1981.
21. Ciarlet, P. G. and J. L. Lions, *Handbook of Numerical Analysis*, Vol. III, North Holland, 1994.
22. Ling, F., D. Jian, and J. M. Jin “Efficient electromagnetic modeling of microstrip structures in multilayer media,” *IEEE Transactions on Microwave Theory and Techniques*, Vol. 47, No. 9, September 1999.
23. Alaybeyi, M. M., J. E. Bracken, J. Y. Lee, V. Raghavan, R. J. Trihy, and R. A. Rohrer, “Exploiting partitioning in asymptotic waveform evaluation (AWE),” *IEEE Conference of Custom Integrated Circuits*, 1571–1574, 1992.
24. Beyene, W. T. and J. E. Schutt-Aine, “Efficient transient simulation of high-speed interconnects characterized by sampled data,” *IEEE Transactions on Components, Package*, Vol. 21, No. 1, 105–114, February 1998.
25. Bracken, J. E., V. Raghavan, and R. A. Rohrer, “Interconnect simulation with asymptotic waveform evaluation (AWE),” *IEEE Transactions on Circuits and Systems-1: Fundamental Theory and Applications*, Vol. 39, No. 11, 869–878, November 1992.
26. Sener, G., L. Alatan, and M. Kuzuoglu, “Use of matrix padé approximation in the analysis of irregularly shaped patch antennas with multiport network model,” *ICEAA International Conference on Electromagnetics in Advance Applications*, 629–631, 2009.